A Consideration of Channel Capacity of Near-field MIMO using Parasitic Elements

[#] Gen Matsui, Hiroshi Hirayama, Nobuyoshi Kikuma, Kunio Sakakibara
Dept. of Computer Science, Nagoya Institute of Technology
Gokiso-cho, Showa-ku, Nagoya, 466-8555, Japan
E-mail hirayama@nitech.ac.jp

1. Introduction

The conventional MIMO systems have a capability of enhancing channel capacity by exploiting multipath environment [1]. Recently, a novel scheme which utilizes MIMO system in near-field region has proposed [2]. In the near-field MIMO system, channel capacity is able to be improved without a multipath, because spherical wave is considered as a superposition of plane waves. It is expected that the near-field MIMO system enables us to realize high-speed short-range wireless communications. We have proposed a novel structure to improve channel capacity using side reflector and back reflector [3]. In this report, we propose a new structure to improve channel capacity using parasitic elements for near-field MIMO.

2. Basic characteristics of the near-field MIMO with parasitic elements

2.1 Calculation model

To maximize channel capacity in eigen-mode transfer, equalizing eigen values of $\mathbf{H}^H\mathbf{H}$ is required, where $\mathbf{H}$ is a channel response matrix and $()^H$ shows conjugate transpose. To achieve this goal, understanding propagation mechanism of the eigen mode is useful. At first, we investigate basic characteristics of near-field MIMO with FDTD simulation. In the conventional MIMO, ray-tracing techniques are often used to calculate channel response matrix. However, ray-tracing techniques assume plane wave propagation. Since the near-field MIMO is used in near-field region and then this assumption is violated, full wave technique is employed.

Figure 1 shows a calculation model for the FDTD simulation. Four half-wavelength dipole antennas are used for TX and RX. Element spacing is set to d[m], thus aperture size A becomes $3d$. Distance between TX and RX antennas is (D). Perfect matched layer (PML) is used as absorption boundary condition. One of the TX element is excited at 2.5GHz. Another TX elements and RX elements are terminated with 50Ω. FDTD simulation is repeated four times by alternating antenna element to excite. Channel response matrix $\mathbf{H} = [h_{ki}]$ is obtained from the complex voltage h_{ki} of the k-th RX element when the i-th TX element is excited.

2.2 Consideration

Eigen values of the $\mathbf{H}^H\mathbf{H}$, which equal to the power of the singular values of $\mathbf{H}$, are shown Table 1. Theoretical values obtained from geometrical optics approximation are also shown in Table 1. The FDTD and the theoretical values for the 1st, 2nd, and 3rd eigen values are similar. However, they are different for the 4th eigen value. It is considered that the 4th eigen value includes effect of mutual coupling between the elements and calculation error of the FDTD simulation caused by reflection from the PML and discretization error.

In the conventional MIMO, eigen beam pattern is used to evaluate eigen beam. Let $\mathbf{e}_t^n$ and $\mathbf{e}_r^n$ be a weight vector of TX and RX for the n-th eigen mode, respectively. $\mathbf{e}_t^n$ and $\mathbf{e}_r^n$ are calculated by singular value decomposition (SVD) of the channel response matrix $\mathbf{H}$:

$$\mathbf{H} = \mathbf{E}_r\mathbf{D}\mathbf{E}_t^H \tag{1}$$

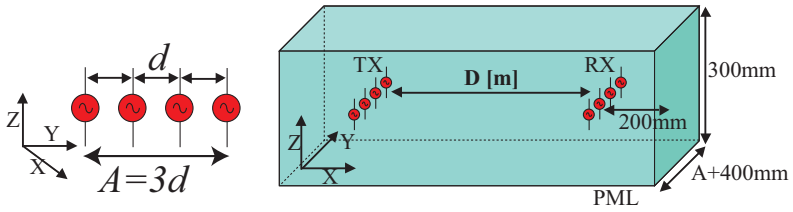

Figure 1: Configuration of the TX and RX antennas and the calculation region for FDTD simulation.

Table 1: Eigenvalues ($d = 0.5\lambda, D = 1m$)

Eigen mode	FDTD [dB]	Theoretical [dB]
1st	0	0
2nd	−14.5	−14.1
3rd	−37.6	−37.9
4th	−54.3	−70.3

Table 2: Phase of TX weight for eigen modes

Eigen mode	Antenna element			
	1st	2nd	3rd	4th
1st	+	+	+	+
2nd	+	+	−	−
3rd	+	−	−	+
4th	+	−	+	−

where

$$\mathbf{E}_t = \left[\mathbf{e}_t^1, \cdots, \mathbf{e}_t^N\right] \tag{2}$$

$$\mathbf{E}_r = \left[\mathbf{e}_r^1, \cdots, \mathbf{e}_r^N\right] \tag{3}$$

$$\mathbf{D} = \mathrm{diag}\left(\sqrt{\lambda_1}, \cdots, \sqrt{\lambda_N}\right) \tag{4}$$

and λ_n is an eigen value of $\mathbf{H}^H\mathbf{H}$. N is a number of antennas. The eigen beam pattern of TX and RX is calculated as an array factor whose weight is $\mathbf{e}_t^n$ and $\mathbf{e}_r^n$, respectively. Figure 2 shows eigen beam patterns of the TX and the RX obtained from the FDTD simulation. Phase of the TX weight is listed in Table 2. In this configuration, the RX antenna is located at 0 degree direction from the TX antenna. According to the 1st eigen mode, all TX elements are excited in-phase, then the eigen beam directs 0 degree direction. However, although the 2nd eigen value is −14.5dB, deep null is formed for 0 degree direction in the 2nd eigen beam. This inconsistency is caused by applying far-field pattern to the near-field region. Therefore, in the near-field MIMO, eigen beam pattern is not adequate to evaluate eigen mode.

Instead of the eigen beam pattern, electric field distribution of eigen mode is conducted to consider eigen mode. Electric Field distribution of n-th eigen mode $E^n(x, y, z)$ is calculated by

$$E^n(x, y, z) = \sum_{i=1}^{N} w_i^n E_i(x, y, z), \tag{5}$$

where w_i^n is the i-th component of the singular vector of n-th singular value, and $E_i(x, y, z)$ is z-component of an electric field distribution when the i-th TX element is excited. Fig. 3 shows the calculation result. We can understand that an azimuth angle of the eigen beam increases in accordance with increase of index of eigen modes to form eigen modes on the RX antennas. Consequently the 2nd, 3rd, and 4th eigen value decreases.

3. Improvement of near-field MIMO

3.1 Proposed Structure

In order to improve channel capacity in MIMO system, not only enlarging signal to noise ratio (SNR) but also equalizing eigen values of channel matrix is important. Figure 4 shows proposed structure for short-range MIMO. This structure consists of half-wavelength dipole antennas and parasitic elements.

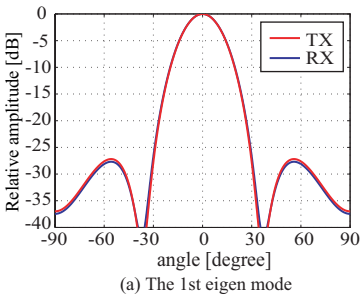

(a) The 1st eigen mode

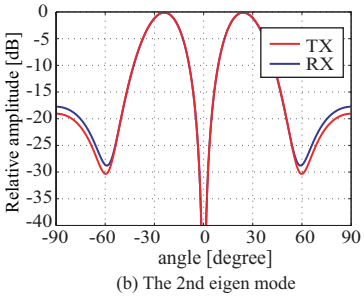

(b) The 2nd eigen mode

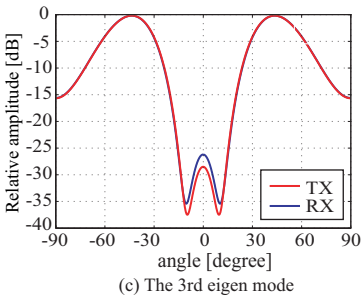

(c) The 3rd eigen mode

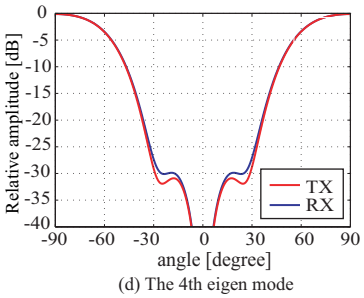

(d) The 4th eigen mode

Figure 2: Far-filed patterns of the eigen modes

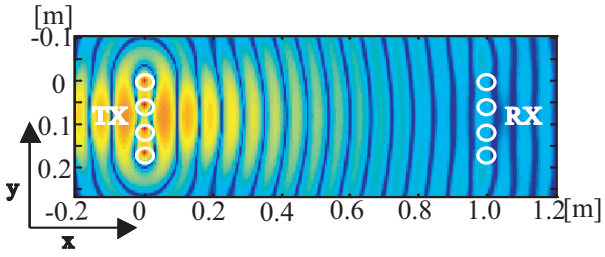

(a)The 1st eigen mode

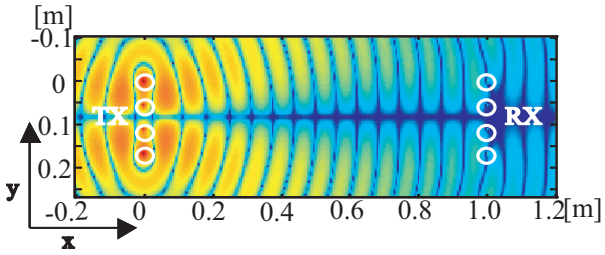

(b)The 2nd eigen mode

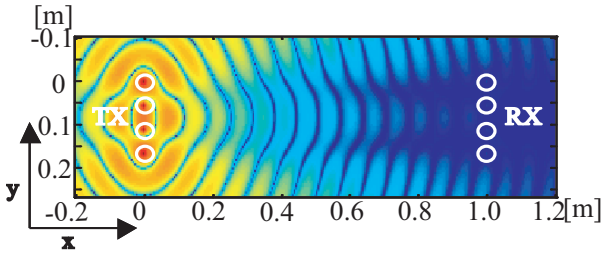

(c)The 3rd eigen mode

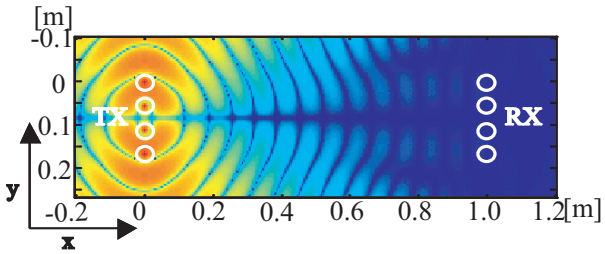

(d)The 4th eigen mode

Figure 3: Electric-field distributions of the eigen modes ($d = 0.5\lambda, D = 1m$)

The parasitic elements whose length is same as half-wavelength are located both endfire directions. Distance between excited element and parasitic element is also d. Thus aperture size including parasitic elements becomes $5d$.

3. 2 Effect of the parasitic elements

Using this structure as TX and RX antenna, FDTD simulation is performed. Fig. 5 shows eigen value distributions as a function of distance between the elements where distance between the TX and RX antennas is $D = 0.6m$. The solid line is for the case of without the parasitic elements, the dashed line is for the case with the parasitic elements. In comparison of the solid line and the dashed line in Fig. 5, it is obvious that the eigen values were increased because of the existence of the parasitic elements. Channel capacity is calculated from these eigen values. Assuming the water-filling theorem, channel capacity for MIMO C_{MIMO} is calculated by

$$C_{MIMO} = \sum_{i=1}^{N} \log_2 (1 + \lambda_i \gamma_i), \tag{6}$$

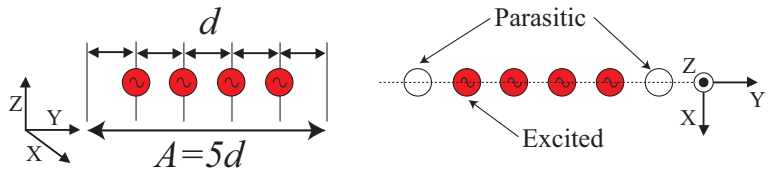

Figure 4: Proposed structure with parasitic elements for near-field MIMO system

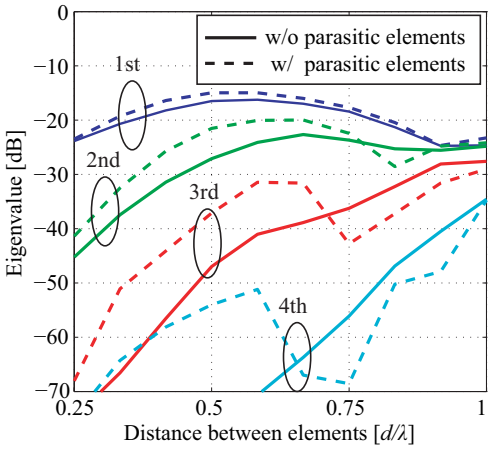

Figure 5: Dependency of the element spacing on the eigen values

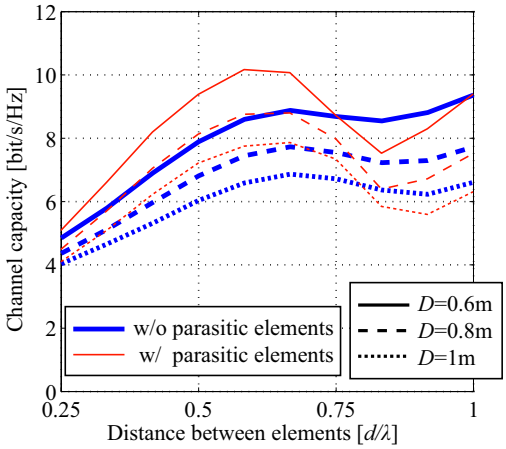

Figure 6: Dependency of the element spacing on the channel capacity

where γ_i is SNR, which is calculated to fulfill

$$\sum_{i=1}^{N} \gamma_i = \gamma_0 \tag{7}$$

with the water-filling theorem. γ_0 is obtained by assuming that TX power is 0dBm and noise power in RX is -100dBm. Figure 6 shows the calculation result. By using the proposed structure, channel capacity increases monotonically with respect to the increase of d/λ. However, when the d/λ become greater than 0.6λ, channel capacity is degraded. It is considered that this is because of grating lobe.

From this result, it is shown that the use of the parasitic element enhances channel capacity. It can be said that the use of the parasitic element has an effect to extend aperture size equivalently without enlarging element space.

4. Conclusion

We proposed an antenna structure to improve channel capacity of near-field MIMO. FDTD simulation demonstrates that the parasitic elements equalize the eigen values. We found that there is an optimal element spacing, which is independent from a distance between TX and RX.

References

[1] Y. Karasawa, “Innovative antennas and propagation studies for MIMO systems in Rician fading,” IEICE Trans on Commun., vol. 4, no. 3. pp. 1102-1111, May. 2005.

[2] N. Honma, K. Nishimori, T. Seki, and M. Mizoguchi, “Short Range MIMO Communication,” Proc.of EuCAP 2009, pp. 1763-1767, Mar. 2009.

[3] H. Hirayama, G. Matsui, N. Kikuma, K. Sakakibara, “Improvement of Channel Capacity of Near-field MIMO,” Proc. of EuCAP 2010, Apr. 2010.